Kinetics of Myosin Subfragment-1-Induced Condensation of G-Actin into Oligomers, Precursors in the Assembly of F-Actin−S_1. Role of the Tightly Bound Metal Ion and ATP Hydrolysis†

Stéphane Fievez, Dominique Pantaloni, and Marie-France Carlier*

Laboratoire d'Enzymologie et Biochimie Structurales, CNRS, Avenue de la Terrasse, 91198 Gif-sur-Yvette Cedex, France

Received May 22, 1997; Revised Manuscript Received July 22, 1997⊗

ABSTRACT: In a low ionic strength buffer and in the absence of free ATP, the interaction of G-actin (G) with myosin subfragment-1 (S_1) leads to the formation of arrowhead-decorated F-actin−S_1 filaments, through a series of elementary steps. The initial formation of GS and G_2S complexes is followed by their condensation into short oligomers. The kinetics of formation of G-actin−S_1 oligomers have been monitored in a stopped-flow apparatus using a combination of light scattering and fluorescence of NBD-labeled actin. Oligomers appear more stable and are formed at a faster rate from MgATP−G-actin than from CaATP−G-actin. The actin-bound ATP is hydrolyzed when oligomers are formed from MgATP−G-actin, not when they are formed from CaATP−G-actin. The formation of oligomers is energetically favored in the presence of cytochalasin D. All data are consistent with the view that the actin−actin interactions which take place upon condensation of GS and G_2S into oligomers are very similar to lateral actin−actin interactions along the short pitch helix of actin filaments, which are involved in actin nucleation. These interactions trigger ATP hydrolysis on actin.

Changes in the organization of actin cytoskeleton are the hallmark of motile responses of the living cells to extracellular stimuli. Actin-binding proteins that are able to nucleate actin assembly are thought to play an important role in these processes. The myosin head or myosin subfragment-1 (S_1) induces the assembly of actin into arrowhead-decorated F-actin−S_1 filaments in low ionic strength solutions in which actin itself remains monomeric. Recent observations (*1*, *2*) showed that some isoform (myosin heavy chain B) of nonmuscle myosin II, the closest homologue of muscle myosin in nonmuscle cells, is found in the cell cortex and in high amount in the lamellipodium of rapidly migrating cells. These results suggest that myosin could induce or assist in the site-directed assembly of a cortical actin scaffold that could contract and cause cell protrusion. Following treatment of cells by cytochalasin B, myosin and actin were colocalized in cortical patches. To understand how cortical actin assembly can be locally controlled by myosin, it is important to characterize the kinetic intermediates of the assembly process.

Myosin subfragment-1 from skeletal muscle is a good model for the actin-binding moiety of all myosins, and its 3D structure is known (*3*). In low ionic strength buffer and in the absence of ATP, S_1 forms tight binary (GS) and ternary G_2S complexes with G-actin (*4*, *5*). The G_2S complex appears as a good functional model of the F-actin−S_1 interface (*5*). The actin−actin interactions in G_2S mimic the longitudinal actin−actin bonds along the long pitch helix in F-actin. At high enough concentration, G_2S and GS condense into oligomers which are kinetic intermediates in the pathway leading to F-actin−S_1. The existence of kinetic intermediates in which different actin−actin bonds are formed offers the opportunity to investigate how the chemical steps of ATP hydrolysis in actin assembly are coupled to the formation of specific actin−actin bonds in the filaments.

The kinetics of formation of G-actin−S_1 oligomers is examined in the present work. Emphasis is given on the role of the divalent metal ion (Ca^{2+} or Mg^{2+}) tightly bound to G-actin in the nucleotide site and the involvement of ATP hydrolysis in oligomer formation.

MATERIALS AND METHODS

Chemicals. NBD-Cl[1] was from Aldrich, α-chymotrypsin from Worthington, cytochalasin D from Sigma, and γ-[^{32}P]-ATP from Amersham.

Proteins. Actin was purified from rabbit muscle acetone powder and isolated as CaATP−G-actin (*7*) by gel filtration through Sephadex G-200 in G buffer (5 mM Tris-Cl^- pH 7.8, containing 0.2 mM DTT, 0.2 mM ATP, 0.1 mM $CaCl_2$, and 0.01% NaN_3). The CaATP−G-actin 1:1 complex was obtained by treatment with Dowex-1-X8 equilibrated in buffer G without ATP (*8*). The MgATP−G-actin 1:1 complex was prepared by adding to the solution of CaATP−G-actin 1:1 complex 0.2 mM EGTA and $MgCl_2$ (1 equiv to actin plus 10 μM) (*9*). The resulting material was used 3 min later. Actin was pyrenyl- (*10*) or NBD-labeled (*11*) as described. The pyrene labels essentially cysteine 374, while 60% of the bound NBD was found attached to lysine 373, other lysines being also labeled (*11*).

† This work was supported in part by the Association Francaise contre les Myopathies (AFM), the Association pour la Recherche contre le Cancer (ARC), the Ligue Nationale Francaise contre le Cancer and a grant from the EEC (Contract CHRX-CT94-0652).

* Corresponding author. Tél: 01 69 82 34 65. Fax: 01 69 82 31 29. E-mail: carlier@lebs.cnrs-gif.fr.

⊗ Abstract published in *Advance ACS Abstracts,* September 15, 1997.

[1] Abbreviations: NBD-Cl, 7-chloro-4 nitrobenzeno-2-oxa-1,3-diazole; NEM, *N*-ethylmaleimide; $S_1(A_1)$ or $S_1(A_2)$, myosin subfragment-1 isoform carrying the A_1 or the A_2 light chain, respectively; MESG, 2-amino-6-mercapto-7 methylpurine ribonucleoside.

S0006-2960(97)01205-1 CCC: $14.00

γ-[^{32}P]−G-actin 1:1 complex was prepared by incubating CaATP−G-actin in G-buffer with γ-[^{32}P]ATP overnight at 0 °C, prior to Dowex treatment.

Myosin was prepared from rabbit muscle (*12*). S_1, obtained by chymotryptic digestion, was resolved into the $S_1(A_1)$ and $S_1(A_2)$ isomers by SP-trisacryl chromatography (*6*).

Protein concentrations were determined spectrophotometrically, using extinction coefficients of 0.617 mg^{-1} cm^2 at 290 nm for actin (*13*) and 0.74 and 0.75 mg^{-1} cm^2 at 278 nm for $S_1(A_1)$ and $S_1(A_2)$, respectively (*14*).

Light Scattering and NBD Fluorescence Measurements. The formation of G-actin−S_1 oligomers was monitored by the increase in intensity of light scattered at 90° angle and 400 nm wavelength and by the change in NBD-actin fluorescence (excitation wavelength, 475 nm; emission wavelength, 530 nm). Experiments were carried out at 20 °C in a Spex fluorolog 2 spectrofluorimeter. Rapid kinetics were performed using a stopped-flow apparatus (DX.17 MV, Applied Photophysics) thermostated at 20 °C and working in the fluorescence mode (excitation wavelength, 475 nm; excitation slit, 0.5 mm). A cut-off filter (KV 490, Schott) was placed on the emission beam. The recorded traces from at least four consecutive shots were averaged and analyzed.

ATPase Measurements. Acid-labile P_i resulting from hydrolysis of the γ-phosphate of actin-bound ATP was measured by extraction of the [^{32}P]-labeled phosphomolybdate complex (*15*). The time courses of ATP hydrolysis and change in NBD fluorescence were followed simultaneously by transferring, at different time intervals, 50 μL aliquots from the sample placed in the spectrofluorimeter cuvette, into the ice-cold ammonium molybdate/1 N HCl quench solution. The time points were identified by occluding the excitation beam at the time the sample was quenched, thus creating a mark on the fluorescence recordings.

RESULTS

MgG-Actin−S_1 Oligomers Are More Stable Than Ca-G-Actin−S_1 Oligomers. In low ionic strength buffer and in the absence of ATP, the binary G-S and ternary (G_2S) complexes of G-actin with S_1 are rapidly formed. The thermodynamics and kinetics of formation of GS and G_2S are very little affected by the nature of the divalent metal ion (Ca^{2+} or Mg^{2+}) bound to G-actin and by the nature of the essential light chain (A_1 or A_2) associated to S_1 heavy chain (*4*, *5*). On the other hand, the condensation of GS and G_2S into oligomers was energetically favored with the $S_1(A_1)$ isoform of S_1 (*6*).

The ability of Mg-actin and Ca-actin to assemble in oligomers in the presence of a saturating amount of $S_1(A_2)$ was compared. Figure 1 shows that the rapid cooperative increase in light scattering indicative of oligomer formation occurred in a range of lower actin concentration when MgATP was bound than when CaATP was bound to G-actin. Nucleation of actin filaments is known to be much easier from MgG-actin than from CaG-actin (*16*−*18*), and the critical concentration for polymerization of Mg-actin is 6-fold lower that that of Ca-actin (*19*), while the rate constants for association of Mg-actin or Ca-actin to filament ends are very similar (*18*). Altogether, these results suggest that while the actin−actin bonds parallel to the actin filament axis, which link the two G-actin molecules in the G_2S complex, are not affected by the nature of the divalent metal ion tightly bound to actin, the more hydrophobic actin−actin bonds formed upon condensation of G_2S into oligomers (*6*), are more stable when MgATP than when CaATP is bound to actin and are probably of the same nature as the actin−actin bonds involved in nucleation of filaments.

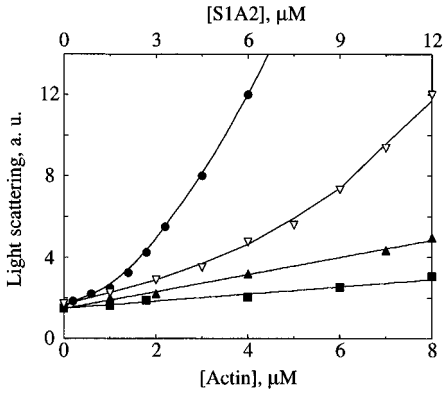

FIGURE 1: Light scattering measurements of the formation of oligomers from CaATP−G-actin or MgATP−G-actin and $S_1(A_2)$. $S_1(A_2)$ at the indicated concentrations (top scale) was added to either CaATP−G-actin (▽) or MgATP−G-actin (●) 1:1 complex at the indicated concentrations (bottom scale) in G_0 buffer. The amount of S_1 added (50% higher than the G-actin) was saturating in all samples. The intensity of light scattered was measured immediately (5 s) after mixing G-actin and S_1. The data shown were collected in a range of actin and S_1 concentrations low enough for the measured increase in light scattering to be kinetically distinct from the subsequent slower increase due to the formation of decorated F-actin−S_1 filaments. The intensity of light scattered by G-actin alone (■) or $S_1(A_2)$ alone (▲) was measured in control samples.

When the above experiment was done with the $S_1(A_1)$ isoform of S_1 instead of $S_1(A_2)$, qualitatively similar data were obtained, in a range of lower actin concentrations.

Kinetics of Oligomer Formation from CaATP−G-Actin or MgATP−G-Actin. While changes in the fluorescence of pyrenyl-actin monitor the formation of GS and G_2S complexes, the fluorescence of NBD-actin is a specific probe for the different actin−actin interactions involved in the formation of actin−S_1 oligomers (*6*). A stopped-flow apparatus was used to monitor the time course of oligomer formation. With Ca-actin and Mg-actin, the fluorescence of NBD-G-actin increased up to 2.1-fold upon mixing with S_1. The maximum extent of fluorescence increase varied cooperatively with either S_1 or G-actin concentration (Figure 2a), but the two partners did not play interchangeable roles in the formation of oligomers. As previously observed for Ca-actin (*6*), a molar ratio of 2 Mg-actins per S_1 was needed to obtain the maximum increase in fluorescence when S_1 was constant while less than 1 M equiv S_1 to actin was sufficient when MgATP−G-actin was kept at a constant concentration.

Typical time courses of NBD fluorescence change are displayed in Figure 2, panels b and c. The increase in fluorescence was faster with Mg-actin than with Ca-actin. In both cases, the kinetics could not be well fitted by a monoexponential process, whether S_1 or G-actin was in large excess over the other reactant.

When oligomers were formed from CaATP−G-actin (Figure 2b), the change in NBD fluorescence was monophasic, and the fluorescence reached at the end of the reaction remained stable for several seconds. Therefore, the formation of oligomers was temporally distinct from the subsequent

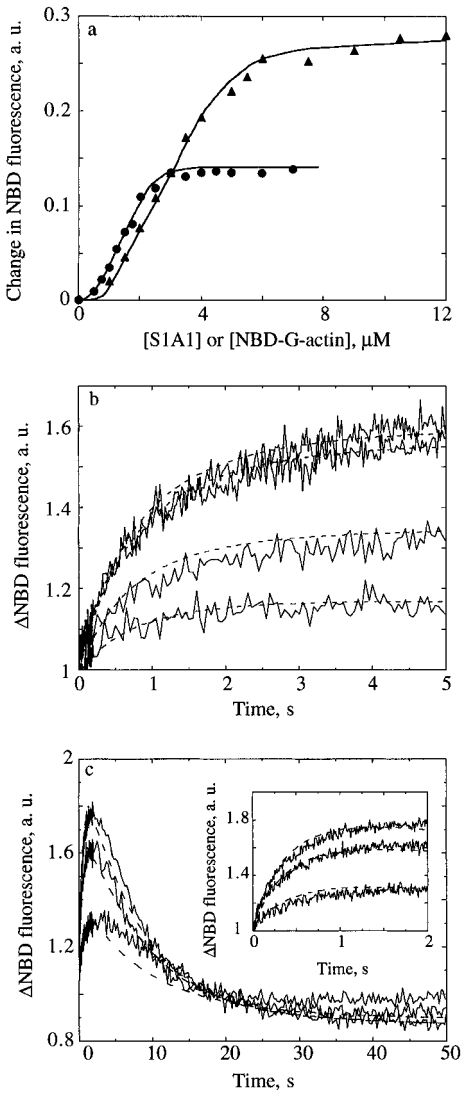

FIGURE 2: Change in NBD actin fluorescence upon formation of oligomers from G-actin and $S_1(A_1)$. (a) Stopped-flow amplitude data. The maximum extent of fluorescence change reached at time 2s following rapid mixing of NBD labeled Mg G-actin with $S_1(A_1)$ was measured in the stopped-flow apparatus. (Closed circles) Dependence of the change in NBD fluorescence on $S_1(A_1)$ concentration, at 3 μM NBD-G-actin. (Closed triangles) NBD-G-actin concentration dependence at 3 μM $S_1(A_1)$. The fluorescence of NBD-G-actin at each concentration is subtracted. (b) Kinetics of oligomer formation from Ca ATP−G-actin and S_1 (A_1). Ca-G-actin (3 μM) was rapidly mixed with $S_1(A_1)$ at 5, 4, 2, and 1.5 μM (top to bottom). (c) Kinetics of oligomer formation from MgG-actin and $S_1(A_1)$. Mg ATP−G-actin was mixed with $S_1(A_1)$ at 5, 2, and 1.25 μM (top to bottom). The fluorescence of G-actin is normalized to 1 in all curves. Noisy curves in panels b and c are experimental traces, and dotted lines are simulated time courses using KINSIM, within Scheme 1 and Scheme 2 and the rate constants and fluorescence parameters given in Table 1.

increase in fluorescence linked to the formation of decorated filaments. In contrast, when oligomers were formed from MgATP−G-actin (Figure 2c), the initial rapid increase in NBD fluorescence was followed by a slower decrease. The fluorescence reached at the end of the slow process was 10% lower than the fluorescence of G-actin. This limit was not visibly reached in a range of high concentration of actin and/or S_1 because the assembly of F-actin−S_1−decorated filaments that follows these initial steps is accompanied by a reincrease in NBD-actin fluorescence, and the beginning of the polymerization reaction obliterates the end of the slow fluorescence decrease that occurs first. The slow decrease in NBD fluorescence was observed with $S_1(A_1)$ as well as with $S_1(A_2)$. No change in light scattering, hence no oligomer dissociation, was associated with it. The slow fluorescence decrease was a first-order process. It also occurred in a range of low Mg-G-actin concentrations at which no oligomers were formed.

Different kinetic schemes were examined for their ability to account for these data using the KINSIM software (*20*) to simulate kinetics of oligomer formation at different actin and S_1 concentrations. The amplitude data suggest that oligomers might be formed by the condensation of G_2S complexes, as described by Scheme 1:

Scheme 1

$$G + S \overset{K}{\rightleftharpoons} GS \qquad \text{(step 1)}$$

$$GS + G \overset{K'}{\rightleftharpoons} G_2S \qquad \text{(step 2)}$$

$$2G_2S \underset{k_{-1}}{\overset{k_{+1}}{\rightleftharpoons}} G_4S_2^* \qquad \text{(step 3)}$$

$$G_2S + GS \underset{k_{-2}}{\overset{k_{+2}}{\rightleftharpoons}} G_3S_2^* \qquad \text{(step 4)}$$

The asterisk (*) indicates that the fluorescence increase is linked to the formation of G_4S_2 and G_3S_2. Steps 1 and 2 were considered as rapid equilibria (*5*) within the time scale of a few seconds within which oligomers were formed. In this scheme, lateral actin−actin interactions are formed in the bimolecular reversible reactions k_{+i}, k_{-i} ($i = 1, 2$) giving rise to an increase in fluorescence of NBD-actin, from the value characteristic of the G, GS, and G_2S species, to a higher value in $G_4S_2^*$ and $G_3S_2^*$. Scheme 1 well described the formation of oligomers from Ca-actin. A simpler scheme in which step 4 was omitted failed to account for the data, because it implied that the formation of oligomers was inhibited at high concentrations of S_1 due to accumulation of GS. This inhibition was not experimentally observed. In the case of Mg-actin, obviously a supplementary slow first-order step subsequent to the formation of G_4S_2 and G_3S_2, appears to occur. The associated decrease in fluorescence of actin was described by a monomolecular conformational change, as follows (Scheme 2):

Scheme 2

$$G_4S_2^* \xrightarrow{k_3} G_4S_2^{**} \qquad \text{(step 5)}$$

$$G_3S_2^* \xrightarrow{k_4} G_3S_2^{**} \qquad \text{(step 6)}$$

The resulting simulated curves are shown together with raw data in Figure 2, panels b (Ca-actin) and c (Mg-actin). All values of rate constants used in the simulation are shown in Table 1.

Because six rate parameters and four fluorescence parameters are involved in Scheme 1, the simulated curves are simply meant to provide an illustration rather than an actual fit to the data. The values of the rate parameters are compatible with the equilibrium data for oligomer formation (Figure 1 and ref 6). The low values of the association rate constants suggest that a conformation change of the con-

Table 1: Rate Constants for Condensation of GS and G_2S in Oligomers and Associated ATP Hydrolysis[a]

	Ca-actin	Mg-actin
K	0.025 μM	0.025 μM
K'	0.005 μM	0.005 μM
k_{+1}	0.35 μM^{-1} s^{-1}	0.7 μM^{-1} s^{-1}
k_{-1}	0.25 s^{-1}	0.3 s^{-1}
k_{+2}	0.45 μM^{-1} s^{-1}	1.2 μM^{-1} s^{-1}
k_{-2}	0.25 s^{-1}	0.15 s^{-1}
k_3	na	0.14 s^{-1}
k_4	na	0.18 s^{-1}
f_1	1	1
f_2	1	1
f_3	1.4	1.7
f_4	2.6	2.7
f_5	na	0.87

[a] K and K' are equilibrium dissociation constants for the formation of GS and G_2S, respectively, (see Scheme 1). k_{+1} and k_{+2} are the association rate constants for the formation of G_4S_2* and G_3S_2* from G_2S and GS complexes. k_{-1} and k_{-2} are the corresponding dissociation rate constants. k_3 and k_4 are the rates of conformation change of G_4S_2* and G_3S_2* into G_4S_2* and G_3S_2*, respectively. f_1 and f_2 are the specific fluorescences of NBD-actin in GS and G_2S, f_3 and f_4 the specific fluorescences of NBD-actin in G_4S_2* and G_3S_2*, f_5 the specific fluorescence of NBD-actin in G_4S_2** and G_3S_2**. The fluorescence of G-actin and of actin in GS and G_2S is normalized to 1 by convention.

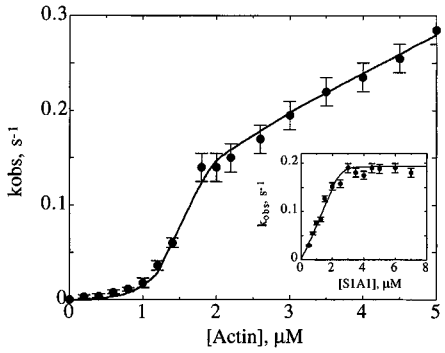

FIGURE 3: Kinetics of the slow conformation change of Mg ATP−G-actin−S_1 oligomers. The slow decrease in NBD-actin fluorescence subsequent to the formation of Mg ATP−G-actin−S_1 oligomers was examined at different concentrations of Mg G-actin and $S_1(A_1)$. Mg G-actin concentration dependence of the first order rate constant at saturating amounts of $S_1(A_1)$ (i.e., 1.5 M equiv per G-actin). (Inset) S_1 concentration dependence of the first order rate constant, at 3 μM Mg G-actin.

densed species follows the bimolecular association reaction. This further complexity was not investigated in detail.

To get more insight into the nature of the slow decrease in NBD fluorescence subsequent to the formation of oligomers from Mg-actin, the dependence of the observed first-order rate constant on actin and S_1 concentration was examined. Figure 3 shows it increased with S_1 in a saturable fashion. The actin concentration dependence of the rate constant reached at saturation by S_1 showed a strong cooperativity. Comparison of this curve with the light-scattering data (Figure 1) indicates that the rate of a slow conformation change linked to the binding of S_1 to actin depends on the degree of actin self-association: the process is 2 orders of magnitude slower in GS and G_2S complexes (k = 0.003 s^{-1}) than in the condensed species (k = 0.25 s^{-1}).

Hydrolysis of ATP Is Enhanced upon Oligomer Assembly from Mg-Actin, Not from Ca-Actin. No hydrolysis of actin-bound ATP occurred upon formation of oligomers from

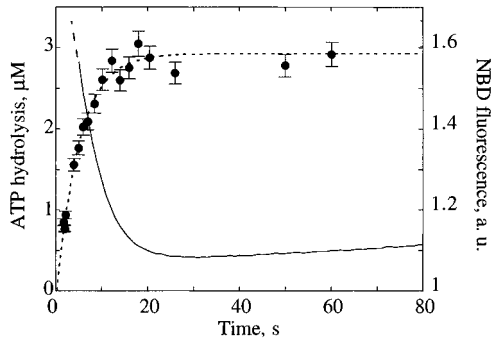

FIGURE 4: Hydrolysis of ATP on Mg-actin is linked to the slow decrease in NBD fluorescence that follows formation of oligomers with S_1. γ-[^{32}P]-Labeled MgATP−G-actin 1:1 complex (3 μM, 80% NBD-labeled) was mixed at time zero with 4.5 μM $S_1(A_1)$. The change in NBD fluorescence was immediately recorded in the spectrofluorimeter (continuous line). The hydrolysis of ATP (acid-labile P_i) was measured in the same sample (symbols and dotted line). The experiment was repeated 3-fold, and resulting cumulated data points are shown.

CaATP-actin and $S_1(A_1)$ or $S_1(A_2)$. In contrast, hydrolysis of ATP occurred and temporally correlated with the slow decrease in NBD fluorescence observed upon interaction of Mg-actin with S_1 (Figure 4). Further measurements of the release of P_i in the medium using purine phosphorylase and MESG as an enzyme-linked assay (*21*) showed that P_i was not released, hence ATP was hydrolyzed by the Mg-actin−S_1 complexes and the product ADP-P_i remained bound to the actin−S_1 complexes (data not shown). Since it had been reported that S_1 binding to G-actin increased the rate of nucleotide dissociation from G-actin (*22*), it was important to determine whether MgATP was hydrolyzed in the actin-bound state upon interaction with S_1 or by S_1 following its dissociation from Mg-actin. To address this issue, light scattering and NBD fluorescence measurements of the interaction of Mg-G-actin with S_1 were carried out using NEM-S_1 (*23*), which cannot hydrolyze ATP following blockage of SH_1. Mg-actin interacted with NEM-S_1 with concomitant changes in NBD fluorescence identical to those observed with underivatized S_1, and actin-bound ATP was hydrolyzed in a similar fashion upon interaction with NEM-S_1, in agreement with ref 24. Under identical ionic conditions, free Mg-ATP (0−5 μM) was not hydrolyzed by NEM-S_1 at the same concentration as in the assays performed in the presence of Mg-ATP-actin. Therefore Mg-ATP is hydrolyzed by actin itself upon interaction of Mg-actin with S_1, and the formation of Mg-ADP-P_i-actin−S_1 complexes is accompanied by a decrease in NBD-actin fluorescence.

The rate of ATP hydrolysis was only 0.003 s^{-1} on the GS and G_2S complexes, in agreement with a recent report (*25*). It was enhanced 70-fold upon oligomerization. Therefore, ATP hydrolysis on Mg-actin is triggered by the new actin−actin contacts formed upon condensation of G_2S. To be specific, in a range of Mg-actin concentrations higher than 3 μM, 95% of the ATP bound to MgG-actin was hydrolyzed within less than 10 s following the addition of 1.5 M equiv S_1. S_1-decorated filaments are assembled, in a subsequent slower step, from MgADP-P_i−S_1 oligomers. The release of P_i occurs later during assembly of decorated F-actin−S_1 filaments (*41*).

Formation of Actin−S_1 Oligomers Is Favored by Cytochalasin D. To understand the nature of actin−actin interactions which take place when oligomers are formed and which lead

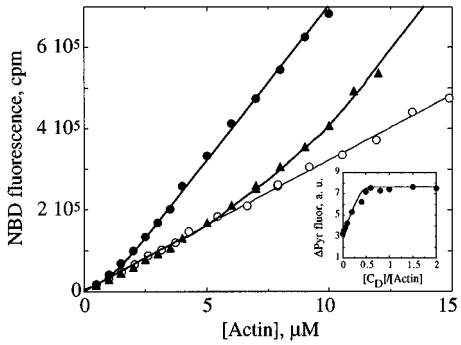

FIGURE 5: Formation of oligomers is energetically favored by cytochalasin D. CaATP−G-actin (100% NBD labeled) at the indicated concentrations, was mixed with 1.5 M equiv $S_1(A_2)$ in the absence (▲) and in the presence (●) of 1 M equiv cytochalasin D. The fluorescence of CaATP−G-actin itself, in the absence of $S_1(A_2)$, was not affected by addition of cytochalasin D (○). (Inset) Cytochalasin D stabilizes G-actin−S_1 oligomers with a 0.5:1 M ratio to G-actin. The formation of oligomers was monitored by the increase in pyrenyl-actin fluorescence upon addition of 1.5 M equiv S_1 to 4 μM CaATP−G-actin, in the presence of the indicated amounts of cytochalasin D (in molar equivalents to G-actin). The fluorescence of pyrenyl-G-actin is normalized to 1.

to the enhancement of ATP hydrolysis on Mg-actin, the effect of cytochalasin D on the formation of oligomers was studied. Cytochalasin D is a drug known to mimic the action of capping proteins (*26*−*28*) and to induce the formation of actin dimers in salt-containing buffers (*29*, *30*). These dimers act as pointed end nuclei (see refs 29 and 31 for a review), similar to gelsolin(actin)$_2$ seeds. Cytochalasin D caused an appreciable increase in the amount of oligomers formed. Light scattering measurements (not shown) and NBD-fluorescence measurements, displayed in Figure 5, show that oligomers are formed at a lower threshold concentration of actin in the presence of cytochalasin D. Under the same conditions, cytochalasin D did not affect the fluorescence of G-actin itself, nor the fluorescence of NBD-actin in GS and G_2S complexes, which are the only actin−S_1 species formed below 1 μM actin. In a range of low concentration of G-actin (<1 μM), the fluorescence titration curves of pyrenyl G-actin by S_1 indicating the formation of GS and G_2S (*4*, *5*) were unaffected by cytochalasin D (data not shown). But at higher G-actin concentration, the increase in fluorescence of pyrenyl-actin linked to the condensation of GS and G_2S was enhanced by cytochalasin D in a dose-dependent fashion (Figure 5, inset). The maximum increase in oligomer formation was observed at a molar ratio of 0.5 cytochalasin D per G-actin, consistent with the notion that the drug stabilizes species in which dimerization of actin is involved. These results confirm that the actin−actin bonds, which are induced by the binding of cytochalasin D to G-actin, are formed upon condensation of GS and G_2S in oligomers.

DISCUSSION

Ca-ATP-actin and Mg-ATP-actin, the latter of which is the physiologically relevant form of actin, have different self-assembly properties and hydrolyze ATP upon polymerization into filaments through different mechanisms. Inducing actin polymerization by myosin subfragment-1 offers an alternative opportunity to examine which actin−actin bond is favored when Mg^{2+} is bound to actin, thus enabling easier nucleation, and to understand how ATP hydrolysis is triggered upon actin self-assembly. Indeed, when actin polymerization is induced by an increase in ionic strength, i.e., by binding of cations to low affinity sites on G-actin, the amount of nuclei formed is extremely small. This low amount is an obstacle in the physical characterization of the structure of the first actin dimer and trimer formed in the prenucleation steps prior to filament growth. On the other hand, when actin polymerization is induced by myosin subfragment-1, a large proportion of the actin molecules are involved in complexes with S_1, which then condense in oligomers, precursors of S_1-decorated filaments. These oligomers are present in solution in mass amounts sufficient for light scattering or changes in fluorescence of labeled actin to be used as physical probes of the protein−protein interactions involved. In addition, it is possible to quantitate ATP hydrolysis potentially associated with specific actin−actin bonds in these oligomers.

We find that G_2S and GS complexes condense more easily into oligomers when Mg^{2+} is bound to actin than when Ca^{2+} is bound, which indicates that the actin−actin bonds formed upon condensation are of the same nature as the ones involved in nuclei formation. Within the view that the hydrophobic actin−actin bonds formed upon condensation of G_2S correspond to the lateral bonds between F-actin subunits in the filament (*6*), the present results indicate that the energetically unfavored, kinetically limiting step in nucleation of actin assembly, would be the formation of the lateral bonds, along the genetic helix of the filament. It is in support of the role of the hydrophobic loop 264−273 in the stabilization of actin−actin bonds along the genetic helix (*32*, *33*). This conclusion is also in agreement with the proposed structure of the gelsolin-(actin)$_2$ pointed end nucleus, in which gelsolin would interact with the two actin subunits, linked by lateral bonds, which form the barbed end of the actin filament. The fluorescence of NBD-actin is also increased upon formation of the gelsolin-(actin)$_2$ ternary complex (*34*, *35*) as it is upon formation of G-actin−S_1 oligomers. Finally, cytochalasin D, which is known to mimic capping/nucleating proteins, lowers the free energy of oligomer formation. This result also supports the view, illustrated in Figure 6, that lateral actin−actin bonds are formed in the oligomerization of GS and G_2S complexes.

Hydrolysis of ATP, without release of inorganic phosphate, occurs on Mg-actin upon its binding to S_1. The hydrolysis proceeds at a slow rate ($k = 0.003$ s^{-1}) in the GS and G_2S complexes and is 70-fold faster in oligomers, suggesting that ATP hydrolysis in filament assembly from MgATP-actin is triggered by the lateral interactions between actin subunits along the genetic helix. Therefore, the reorientation of the hydrophobic loop 264−273 of actin that is associated with the establishment of cross-strand interactions is linked to ATP hydrolysis. This view corroborates recent results by Feng et al. (*36*) showing that a change in environment of this loop occurs upon polymerization of actin and that binding of S_1 to actin subdomains 1 and 2 affects the environment of the loop between subdomains 3 and 4. Our results also agree with the recent report that ATP is hydrolyzed on one of the two G-actin molecules in the gelsolin(actin)$_2$ complex (*37*) and possibly on cytochalasin D-induced dimers (*29*, *31*). Altogether, these results lead to the important conclusion that ATP is hydrolyzed upon nucleation of Mg-actin, without release of Pi. The release of Pi requires actin subunits to be fully buried in a helical polymer (*41*). When CaATP is

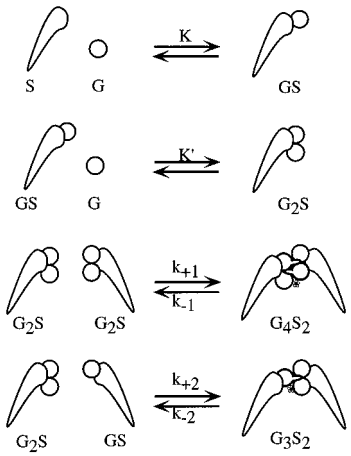

FIGURE 6: Schematic representation of the condensation of GS and G_2S in oligomers. The actin−actin bonds in G_2S are similar to longitudinal actin−actin bonds in the actin filaments. The actin−actin bonds that are formed upon condensation of G_2S and GS are similar to lateral actin−actin bonds along the genetic helix of the actin filament. The extension of the hydrophobic loop associated with the formation of oligomers is depicted on the diagram, as well as the binding of cytochalasin D (daisy symbol).

bound to G-actin, in contrast, hydrolysis of ATP occurs more slowly and subsequent to the incorporation of actin in the decorated F-actin−S_1 filament, a feature identical to the hydrolysis of ATP in salt-induced assembly of Ca-F-actin (*38*).

The fact that Ca-ATP-actin has a higher critical concentration for polymerization than Mg-actin appears linked to weaker lateral bonds in Ca-F-actin. Interestingly, no difference was found in the rigidity of filaments assembled from either Ca-actin or Mg-actin (*39*, *40*), while a large difference in torsional rigidity has recently been reported (*40*). This difference in the torsional rigidity may be in relation with the structural difference in the lateral bonds in Ca-F-actin and Mg-F-actin.

REFERENCES

1. Maupin, P., Phillips, C. L., Adelstein, R. S., and Pollard, T. D. (1994) *J. Cell Sci. 107*, 3077−3090.
2. Kelley, C. A., Sellers, J. R., Gard, D. L., Bui, D., Adelstein, R. S., and Baines, I. C. (1996) *J. Cell Biol. 134*, 675−685.
3. Rayment, I., Ripniewski, W. R., Schmidt-Bäse, K., Smith, R., and Tomchick, D. R., (1993) Science 261, 50−58.
4. Valentin-Ranc, C., Combeau, C., Carlier, M.-F., and Pantaloni, D. (1991) *J. Biol. Chem. 266*, 17871−17879.
5. Blanchoin, L., Fievez, S., Travers, F., Carlier, M.-F., and Pantaloni, D. (1995) *J. Biol. Chem. 270*, 7125−7133.
6. Valentin-Ranc, C., and Carlier, M.-F. (1992) *J. Biol. Chem. 267*, 21543−21550.
7. McLean-Fletcher, S., and Pollard, T. D. (1980) *Biochem. Biophys. Res. Commun. 96*, 18−27.
8. Mockrin, S., and Korn, E. D. (1980) *Biochemistry 19*, 5358−5363.
9. Carlier, M.-F., Pantaloni, D., and Korn, E. D. (1986) *J. Biol. Chem. 261*, 10785−10792.
10. Kouyama, T., and Mihashi, K. (1981) *Eur. J. Biochem. 114*, 33−38.
11. Detmers, P., Weber, A., Elzinga, M., and Stephens, R. E. (1981) *J. Biol. Chem. 256*, 99−105.
12. Offer, G., Moos, C., and Starr, R. (1973) *J. Mol. Biol. 74*, 653−676.
13. Gordon, D. J., Yang, Y. Z., and Korn, E. D. (1976) *J. Biol. Chem. 251*, 7474−7479.
14. Margossian, S. S., and Lowey, S. (1982) *Methods Enzymol. 85*, 55−71.
15. Carlier, M.-F., Pantaloni, D., and Korn, E. D. (1984) *J. Biol. Chem. 259*, 9983−9986.
16. Tobacman, L. S., and Korn, E. D. (1983) *J. Biol. Chem. 258*, 3207−3214.
17. Cooper, J. A., Buhle, E. L., Jr., Walker, S. B., Tsong, T. Y., and Pollard, T. D. (1983) *Biochemistry 22*, 2193−2202.
18. Carlier, M.-F., Pantaloni, D., and Korn, E. D. (1986) *J. Biol. Chem. 261*, 10785−10792.
19. Carlier, M.-F. (1991) *J. Biol. Chem. 266*, 1−4.
20. Barshop, B. A., Wrenn, R. F., and Frieden, C. (1983) *Anal. Biochem. 130*, 1−11.
21. Melki, R., Fievez, S., and Carlier, M.-F. (1996) *Biochemistry 35*, 12038−12045.
22. Kasprzak, A. A. (1993) *J. Biol. Chem. 268*, 13261−13266.
23. Reisler, E. (1982) *Methods Enzymol. 85*, 84−93.
24. Combeau, C., Didry, D., and Carlier, M.-F. (1992) *J. Biol. Chem. 267*, 14038−14046.
25. Kasprzak, A. A. (1994) *Biochemistry 33*, 12456−12462.
26. Brown, S. S., and Spudich, J. A. (1981) *J. Cell Biol. 88*, 487−491.
27. Flanagan, M. D., and Lin, S. (1980) *J. Biol. Chem. 255*, 835−838.
28. Carlier, M.-F., Criquet, P., Pantaloni, D., and Korn, E. D. (1986) *J. Biol. Chem. 261*, 2041−2049.
29. Goddette, D. W., and Frieden, C. (1986) *J. Biol. Chem. 261*, 15974−15980.
30. Goddette, D. W., Uberbacher, E. C., Bunick, G. J., and Frieden, C. (1986) *J. Biol. Chem. 261*, 2605−2609.
31. Cooper, J. A. (1987) *J. Cell Biol. 105*, 1473−1478.
32. Lorenz, M., Popp, D., and Holmes, K. C. (1993) *J. Mol. Biol. 234*, 826−836.
33. Chen, X., Cook, R. K., and Rubenstein, P. A. (1993) *J. Cell Biol. 123*, 1185−1195.
34. Bryan, J., and Kurth, M. C. (1984) *J. Biol. Chem. 259*, 7480−7487.
35. Coué, M., and Korn, E. D. (1985) *J. Biol. Chem. 260*, 15033−15041.
36. Feng, L., Kim, E., Lee, W.-L., Miller, C. J., Kuang, B., Reisler, E., and Rubenstein, P. A. (1997) *J. Biol. Chem. 272*, 16829−16837.
37. Laham, L. E., Lamb, J. A., Allen, P. G., and Janmey, P. A. (1993) *J. Biol. Chem. 268*, 14202−14207.
38. Carlier, M. F., Pantaloni, D., and Korn, E. D. (1987) *J. Biol. Chem. 262*, 3052−3059.
39. Isambert, H., Venier, P., Maggs, A. C., Fattoum, A., Kassab, R., Pantaloni, D., and Carlier, M.-F. (1995) *J. Biol. Chem. 270*, 11437−11444.
40. Yasuda, R., Miyata, H., and Kinosita, K., Jr. (1996) *J. Mol. Biol. 263*, 227−236.
41. Fievez, S., Carlier, M.-F., and Pantaloni, D. (1997) *Biochemistry 36*, 11843−11850.

BI971205W